EUROPEAN JOURNAL OF BIOMEDICAL AND PHARMACEUTICAL SCIENCES
http://www.ejbps.com

ISSN 2349-8870
Volume: 7
Issue: 9
19-31
Year: 2020

COMPUTATIONAL DESIGN OF NANOPARTICLES FOR DETECTION OF CLINICALLY RELEVANT PEPTIDES FOR THE ULTRA-RARE LIVER DISEASE CREIGLER-NAJJAR SYNDROME

Anthony E. Soroh*[1,2], Berezi E. P.[1], Kal Karim[2], Mirrin E.[1] and Berezi P. K.[3]

[1]Department of Chemistry, School of Science, Isaac Jasper Boro College of Education, Sagbama. Bayelsa State, Nigeria.
[2]Department of Chemistry, University of Leicester, United Kingdom.
[3]Department of Biology, School of Science, Isaac Jasper Boro College of Education, Sagbama. Bayelsa State, Nigeria.

***Corresponding Author: Anthony E. Soroh**
Department of Chemistry, School of Science, Isaac Jasper Boro College of Education, Sagbama. Bayelsa State, Nigeria.

Article Received on 02/07/2020 **Article Revised on 23/07/2020** **Article Accepted on 12/08/2020**

ABSTRACT
The present study focused on the selection of a suitable monomer that can be used for the development of a molecular imprinted polymer (MIP) for the identification of the rare liver disease Creigler-Najjar Syndrome (CNS). The computational approach was used to screen eight (8) selected monomers which were initially minimized along with 6 clinically relevant peptides of different sequences using the Sybyl 7.3 software. The Leapfrog results showed that 3-methacrylamido-1-aminium gave the highest value and was the preferred functional monomer amongst the selected monomers. It exhibited the highest binding scores with all the six peptides. Recorded values were -72.56 kcal/mol, -64.77 kcal/mol, -68.68 kcal/mol, -77.38 kcal/mol, -108.45 kcal/mol and -88.14 kcal/mol. This functional monomer showed promising properties as it exhibited strong hydrogen bonding with the six peptides.

KEYWORDS: Nanoparticles, Creigler-Najjar Syndrome, Functional Monomers, Leapfrog, Binding Scores, Peptides.

INTRODUCTION
Basically, molecular imprinted polymers are prepared by the polymerisation of a suitable monomer and a cross-linker agent in the presence of a template molecule. The template is usually removed after polymerization from the matrix leaving cavities that fits the size and shape of the compound.[1] These polymers could have variety of recognition properties when applied analytically; such as solid phase extraction[2], binding assay[3], chemical sensor[4,5], chromatographic separation[6,7], chemical synthesis.[8] To improve the properties of the MIP computer –aided studies have been employed as a quick method.[9] In some researches[10,11,12], a pool of functional monomers were used to assign and screen against the target template molecule and properly managed to improve the selective property of the MIP with the aid of computational simulation.

Crigler Najjar Syndrome (CNS) was first discovered in 1952 by Crigler and Najjar.[13] It is a genetic mutation and are found in both genders.[14,15] Crigler Najjar Syndrome are of two types, the Type I and Type II. It is predominant among the Amish, Mennonite and in the Sub Mediterranean region of Tunisia.[16,17] This is due to the absence of uridine disphosphate glucuronosyltransferase (UGTIAI). This is so, as glucuronidation is very important for the biliary removal of bilirubin and UGTIAI.[18] It is a metabolic disorder as the activity of UGTIAI can be changed by nucleotide polymorphism which could be completely absent or only about 10% to 30% in patients with Crigler Najjai Type1, Type2 and Gilbert's syndrome.[19]

Crigler Najja Syndrome Type I(CN-1) is a diseased condition in which the body cannot convert unconjugated bilirubin to the conjugated bilirubin due to the complete absence of the enzyme UGTIAI. This condition is hereditary as shown in Figure1.[20] It can manifest within 7 days after birth, with the development of very high level of bilirubin. These kernicterus when not attended to medically could result to bilirubin encephalopathy and can lead to death of the child within 18 months. For Crigler Najjar Syndrome Type I (CN-1) the serum bilirubin level is between 340 - 850 µmol/L. There is an estimated occurrence ratio of 1:1,000.000 per birth.

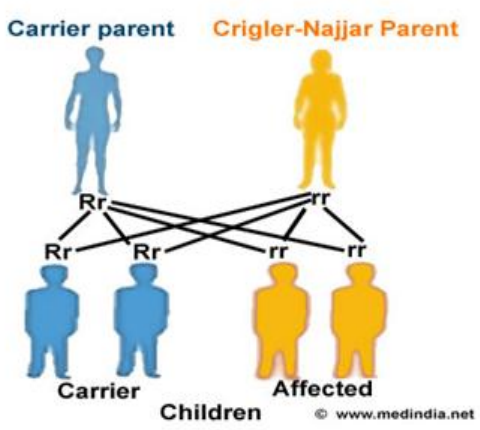

Fig 1: Hereditary traits from Parents to Children.

Crigler Najjar Syndrome Type II (CN-2) are caused by limited amount of uridine diphosphate - glucuronsoyl - transferase. It is usually not as serious as the Type I. It has a serum bilirubin level of below 350 umol/L. The bile of persons having the Type II has both the mono and diglucuronides bilirubin in smaller quantities. The disease results from genetic mutation of the exons located in the UGT1. This is shown in Fig.2.[21]

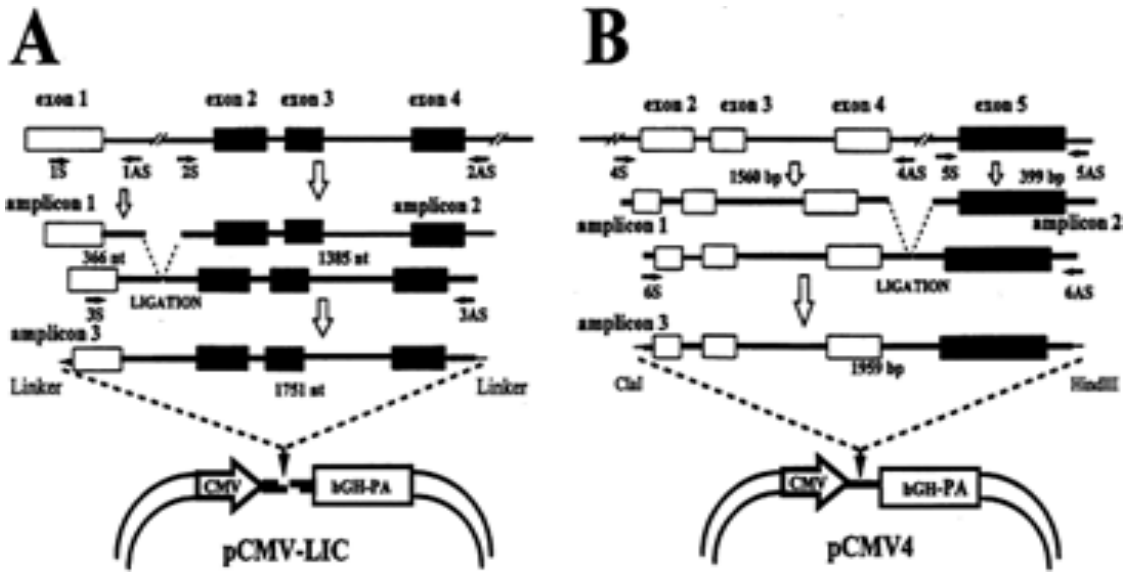

Fig. 2 Splice- site mutation.

The UGT1A1 gene are particularly responsible for the production of the enzyme UDP-glucuronosyltransferases that are involved in the glucuronidation reaction. The bilirubin uridine diphosphate glucuronosyl transferase (bilirubin-UGT) enzyme are proteins produced by UGT1A1. This is the only enzyme that glucuronidates bilirubin, a substance produced as a result of the breaking down of the red blood cells and are found in the liver. UDPGT plays a very unique role in the human body which include its ability to bind with xenobiotics and endogenous compounds that are toxic to the body, by so doing, they are easily excreted from the body. UDPGT is very important in the conversion of glucuronidate bilirubin IX-alpha to form both the IX-alpha-C8 and IX-alpha-C12 monoconjugates and diconjugate, it also speed up the glucuronidation of 17beta-estradiol, 17alpha-ethinylestradiol, 1-hydroxypyrene, 4-methylumbelliferone, 1-naphthol, paranitrophenol, scopoletin, and umbelliferone. Its actual mode of action generally is illustrated in Figure 3.[22] The UGT1A complex locus are made up of both the first and the terminal exons which are capable of producing 3 very abundant exons with 2 varying terminal exons. There are also 27 possible mRNA isoforms of which there are nine (9) known functionally active polypeptides (UGT1A1, 1A3, 1A4, 1A5, 1A6, 1A7, 1A8, 1A9 and 1A10) called isoforms 1.[23]

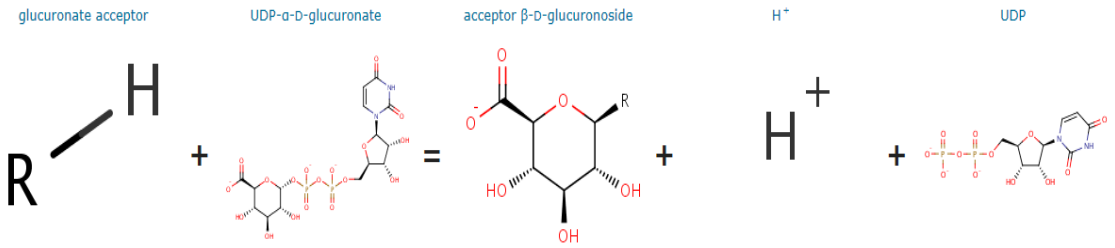

Fig 3: Mode of action of the UGT1A!.

Bilirubin are produced by the metabolism of the blood heme as a result of ring opening as illustrated in Fig 4.[23] The level of bilirubin in serum are ncreased under certain medical situations.[24]

The total bilirubin levels are the sum of its conjugated and unconjugated states, which is the levels of bilirubin before and after hepatic activity. The acceptable level for total bilirubin is between 5 - 19 µmol/L in blood, an increase above this value result in pathological condition more especially in neonate which may cause kennicerus been that the brain tissues are prone to its harmful effects, while other complications include Dublin - Johnson Syndrome, Rotor Syndrome and Jaundice.[25,26,27]

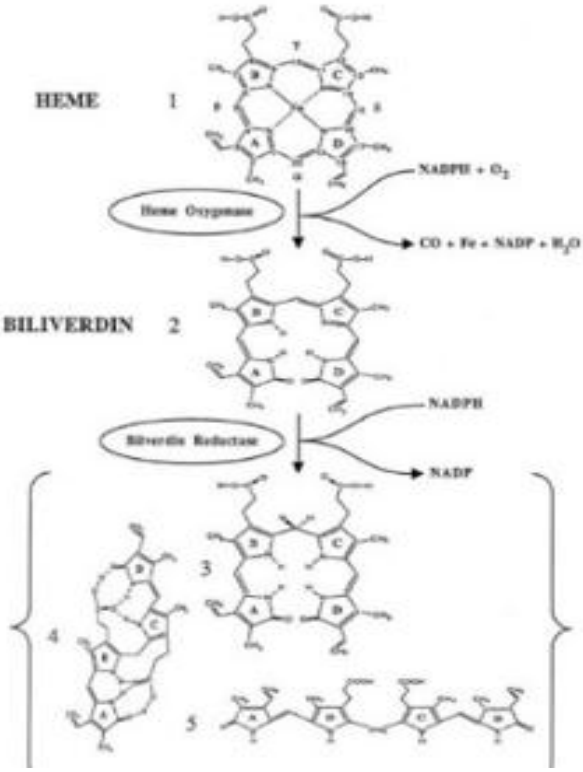

Fig 4: Hemoglobin Metabolism.

Due to adverse complication resulting from poor detection and management, there is the need for the development of a reliable detector with properties similar to the biological receptors. This paper is focused on the production of suitable Molecularly Imprinted Polymers (MIP) based on computational design.

MATERIALS AND METHOD

The modelling were performed using the Sybyl 7.3 Software package on a dedicated HP Elite Desk G1 Tower PC running CentOS Linux 7.

Six peptides (target molecules) were used. They are as follows

- Peptide 1: CLSVSPGGQWLVSGSD (P1705418)
- Peptide 2: CGHLSQGVQWSLLLAVPSR(P1705419)
- Peptide 3: CGTVGFGGIGSLIDFILISR (P1803104)
- Peptide 4: CQIVGPSDGSSYIIDYYGTR (P1803105)
- Peptide 5: CGLTSPQVYDNQEPLREEDSDFILTEGD (P1803106)
- Peptide 6: CLTLTYGDSTVTANGSSSSHTASTSLEGSR (P1803107)

All the peptides had cysteine added at the end of each peptide (N-terminus) in order to attach via SH coupling to the glass beads, the other end being the C-terminus. The functional monomers are as listed below with their structures presented in Figs. 5 -12

- Acrylic acid (AAc)
- N-3-aminopropyl methacrylamide (APM
- N-t-butylacrylamide (TBAm)
- N-Phenylacrylamide
- N,N-methylenebisacrylamide (BIS)
- N-isopropylacrylamide (NIPAm)
- Acrylate

3-Methacrylamidopropan-1-aminium

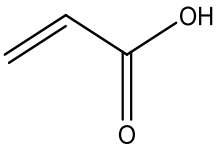

Fig.5 Acrylic acid (AAc) MW 72.06g

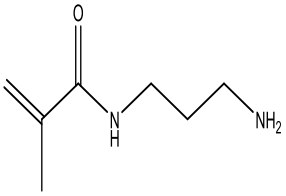

Fig.6 N-3-aminopropylmethacrylamide (APM) MW. 142.11g

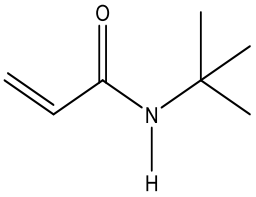

Fig7. N-t-butylacrylamide (TBAm)

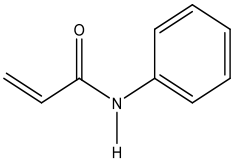

Fig.8 N-phenylacrylamide MW 147.17g

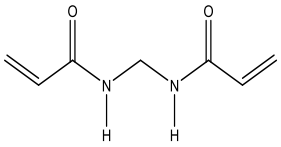

Fig.9 N,N-methylenebisacrylamide (BIS) MW 154.17g

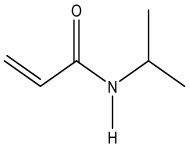

Fig.10 N-isopropylacrylamide (NIPAm) MW 113.16

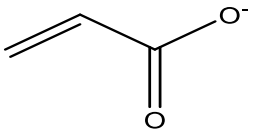

Fig.11 Acrylate MW 71.06g

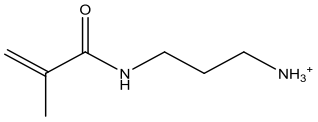

Fig. 12 3-Methacrmidopropan-1-aminium MW 143.12g.

The procedure was carried using the method adapted by Piletisky.[27]

MINIMIZATION OF FUNCTIONAL MONOMERS

The minimization energies of the eight functional monomers are summarised in Table 1. showing the conformational stable structure to the functional monomers. These was very important in the synthesis of the molecularly imprinted polymers as it ensured higher affinity, selectivity and greater cavity formation with better recognition.

Table 1: Minimization Energies of Functional Monomers.

S. NO	NAME OF FUNCTIONAL MONOMERS	MOLECULAR WEIGHT g/mol	MINIMIZED STRUCTURES	MINIMIZATION ENERGY (KCAL/MOL)
1.	Acrylic acid (AAc)	72.06	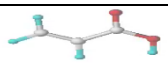	-7,78
2.	N-3-aminopropylacrylamide ((Apm)	142.12	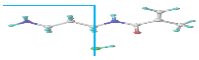	-0.24
3.	N-isopropylacrylamide (Nipam)	113.16	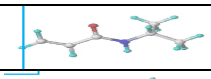	-11.73
4.	N-phenylacrylamide (Npam)	147.17	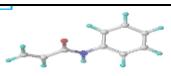	-5.98
5.	N,N-methylenebisacrylamide (BIS)	154.17	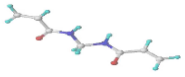	-26.05
6.	N-t-butylacrylamide (Tbam)	127.18	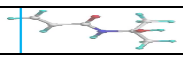	-14.46

7.	Acrylate	71.06g	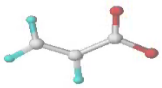	24.76
8.	3-Methacrylamido-1-aminium	143.12		19.57

MINIMIZATION OF PEPTIDES

The six peptides (target molecules or templates) were minimized and further subjected to dynamics and second minimization. This were done to ensure that a more stable conformation for the six peptides were obtained prior to the formation of the template monomer complex. This was done to achieve greater hydrogen bonding within the peptides and formation of non-covalent bonds which played crucial role in the polymerization process resulting in high affinity, selectively and formation of better recognition cavities. The results of the above procedures are all presented in Table 2. It was also known that the structures of the six peptides before minimization were all linear but at the end of the second minimization, they were all folded as shown in Figures 13-18.

Table 2: Results of minimization, dynamics and second minimization on the six Peptides.

S/No	NAMES OF PEPTIDE	1ST MINIMIZATION ENERGY (KCAL/MOL)	DYNAMICS ENERGY VALUES (KCAL/MOL)	2ND MINIMIZATION ENERGY (KCAL/MOL)
1.	PEPTIDE 1 ZY (P1705418)	-13.200	-91.555	-278.901
2.	PEPTIDE 2 ZY (P1705419)	-142.433	-80.516	-320-264
3.	PEPTIDE 3 ZY (P1803104)	-150.182	-81.189	-335.230
4.	PEPTIDE 4 ZY (P1803195)	-207.226	-180.764	-444.955
5.	PEPTIDE 5 ZY (P1803106)	-240.494	-47.402	-427.631
6.	PEPTIDE 6 ZY (P1803107)	-204.760	-160.985	-486.772

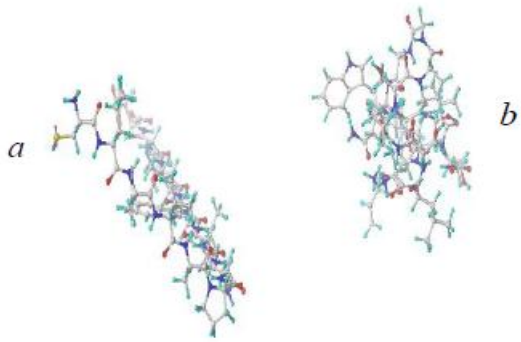

Fig. 13: Peptide ZY (a) before minimization and (b) after second minimization.

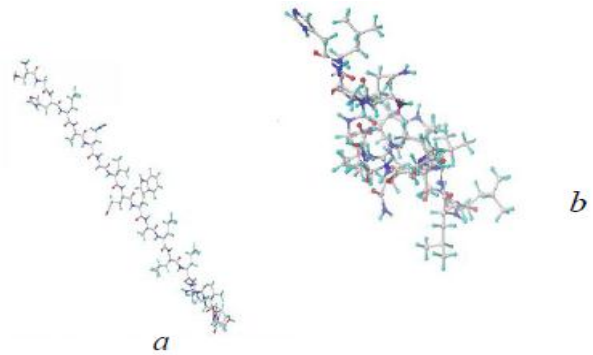

Fig. 14: Peptide2ZY (a) before first minimization and (b) after second minimization.

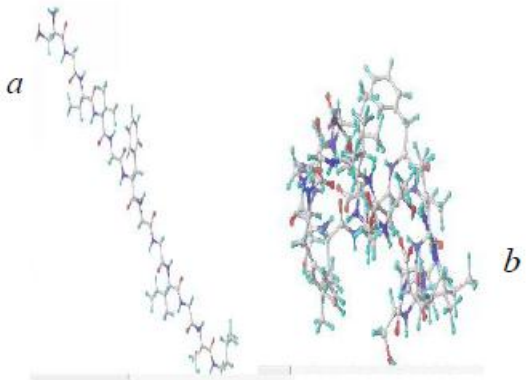

Fig. 15: Peptide 3ZY (a) before first minimization and (b) after second minimization.

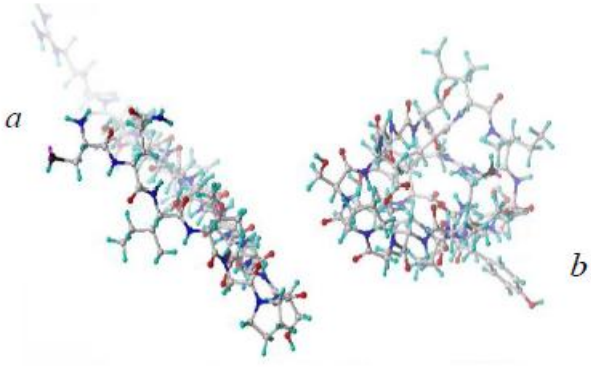

Fig. 16: Peptide 4ZY (a) before first minimization and (b) after second minimization.

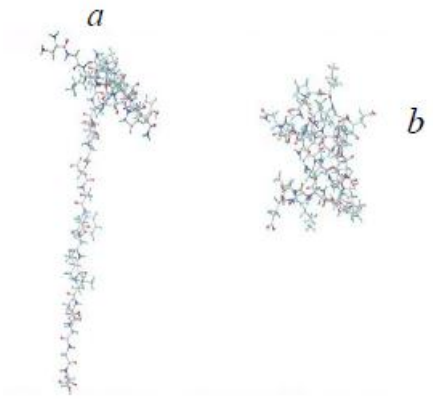

Fig. 17: Peptide 5ZY (a) before first minimization and (b) after second minimization

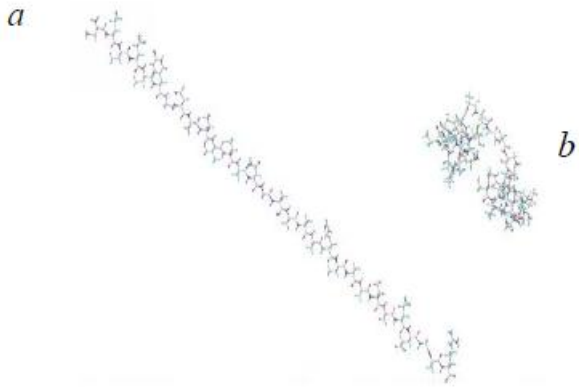

Fig. 18: Peptide 6ZY (a) before first minimization and (b) after second minimization.

ANALYSIS FROM BACHEM PEPTIDE CALCULATOR

The molecular weight of all the peptides and their net ionic charges were determined using the Bachem Peptide Calculator. The results for the six peptides are shown in Tables 3, which provides a better understanding about the Leapfrog procedures whose result would be discussed later.

From the results it was observed that, there are four basic, one acidic and one neutral peptides which would play an important role in its affinity for the functional monomers.

Table 3: The molecular weight and the net ionic charges of the Peptides.

S/No	Names of peptide	Sequence	Nos of amino acids	Molecular weight g/mol	Net ionic charge
1.	PEPTIDE 1 ZY (P1705418)	CLSVSPGGQWLVSGSD	16	1591.76	-1.0
2.	PEPTIDE 2 ZY (P1705419)	CGHLSQGVQWSLLLAVPSR	19	2051.40	+1.0
3.	PEPTIDE 3 ZY (P1803104)	CGTVGFGGIGSLIDFILISR	20	2025.40	0.0
4.	PEPTIDE 4 ZY (P1803105)	CQIVGPSDGSSYIIDYYGTR	20	2194.41	-1.0
5.	PEPTIDE 5 ZY (P1803106)	CGLTSPQVYDNQEPLREEDSDFILTEGD	28	371.36	-7.0
6.	PEPTIDE 6 ZY (P1803107)	CLTLTYGDSTVTANGSSSSHTASTSLEGSR	30	2991.15	-1.0

LEAGFROG RESULTS WITH THE 8 FUNCTIONAL MONOMERS

Table 4: Summary of leapfrog results with Peptide 1.

SNO	NAME OF MONOMER	STRUCTURE OF MONOMER	BINDING SCORES K/CAL/MOL
1	3-methacrylamido-1-aminium	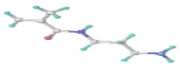	-72.56
2	N-3-aminopropylmethacrylamide	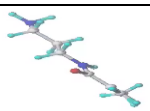	-44.02
3	N,N-methylenebisacrylamide		-34.57

4	N-t-butylacrylamide		-33.08
5	N-phenylacrylamide	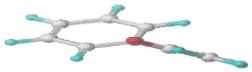	-26.28
6	N-isopropylacrylamide	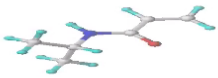	-22.87

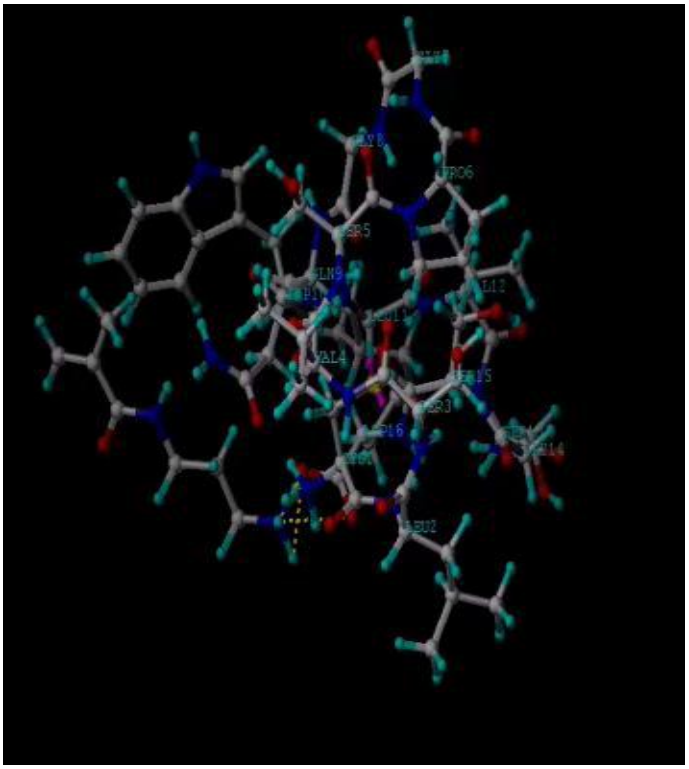

Fig. 19: Peptide 1 in hydrogen bonding with 3-methacrylamido-1-aminium.

Table 5: Summary of Leapfrog results for Peptide2.

S. NO	NAME OF MONOMER	STRUCTURE OF MONOMER	BINDING SCORES K/CAL/MOL
1	3-methacrylamido-1-aminium	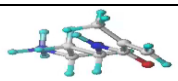	-64.77
2	N-3-aminopropylmethacrylamide	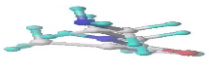	-38.26
3	N,N-methylenebisacrylamide	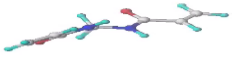	-31.42
4	N-phenylacrylamide		-24.44
5	N-isopropylacrylamide	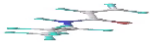	-21.37
6	N-t-butylacrylamide		-21.28

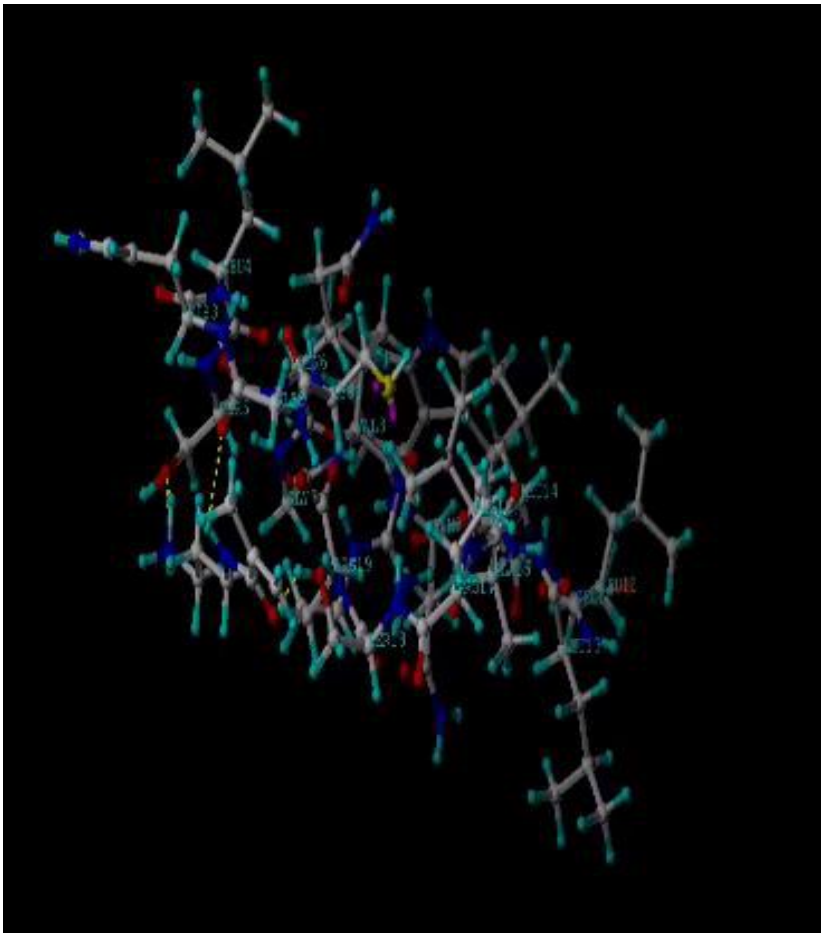

Fig 20: Peptide 2 in hydrogen bonding with 3-methacrylamido-1-aminium.

Table 6: Summary of the Leapfrog on Peptide 3.

SNO	NAME OF MONOMER	STRUCTURE OF MONOMER	BINDING SCORES K/CAL/MOL
1	3-methacrylamido-1-aminium		-68.68
2	N,N-methylenebisacrylamide	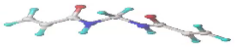	-48.80
3	N-3-aminopropylmethacrylamide	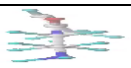	-33.78
4	N-isopropylacrylamide	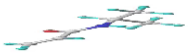	-25.38
5	N-phenylacrylamide	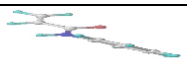	-23.37
6	N-t-butylacrylamide	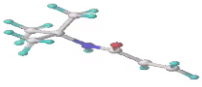	-22.43

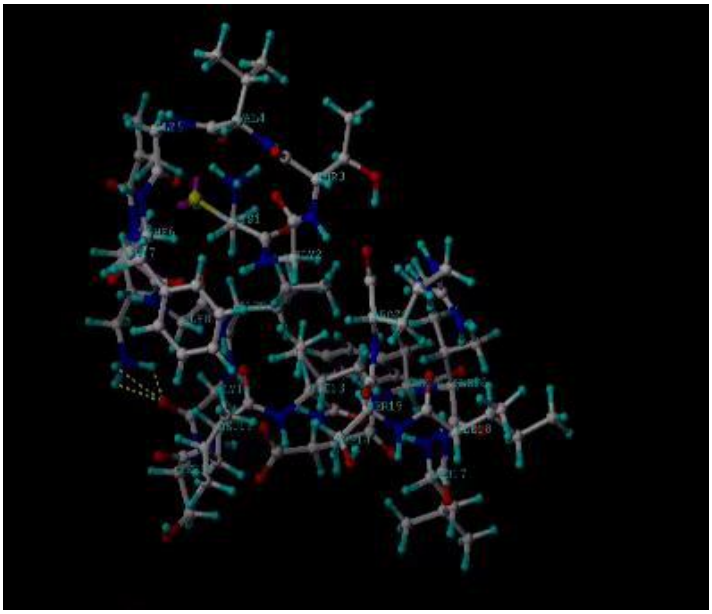

Fig 21: Peptide 3 in hydrogen bonding with 3-methacrylamido-1-aminium.

Table7: Summary of the Leapfrog on Peptide 4.

SNO	NAME OF MONOMER	STRUCTURE OF MONOMER	BINDING SCORES K/CAL/MOL
1	**3-methacrylamido-1-aminium**	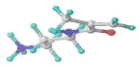	-77.38
2	**N,N-methylenebisacrylamide**	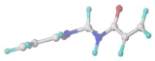	-38.50
3	**N-3-aminopropylmethacrylamide**		-36.57
4	**N-isopropylacrylamide**	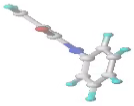	-26.51
5	**N-phenylacrylamide**	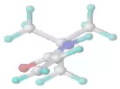	-23.48
6	**N-t-butylacrylamide**		-20.95

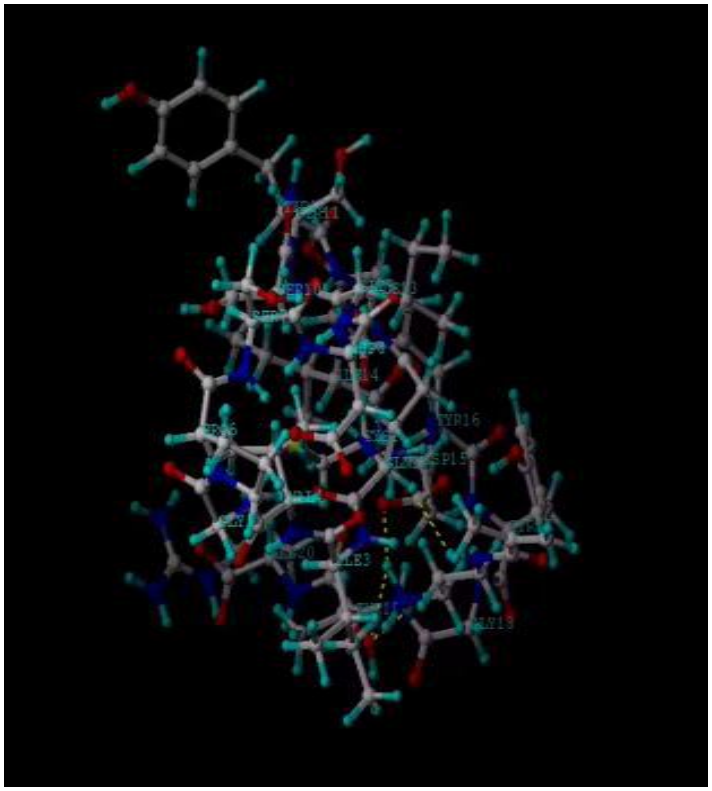

Fig. 22: Peptide 4 in hydrogen bonding with 3-methacrylamido-1-aminium.

Table 8: Summary of the Leapfrog on Peptide 5.

SNO	NAME OF MONOMER	STRUCTURE OF MONOMER	BINDING SCORES K/CAL/MOL
1	3-methacrylamido-1-aminium	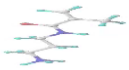	-108.45
2	N,N-methylenebisacrylamide		-41.90
3	N-3-aminopropylmethacrylamide		-38.85
4	N-phenylacrylamide	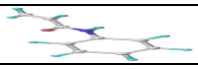	-30.03
5	N-isopropylacrylamide	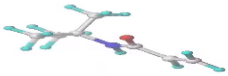	-28.03
6	N-t-butylacrylamide	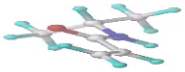	-27.82

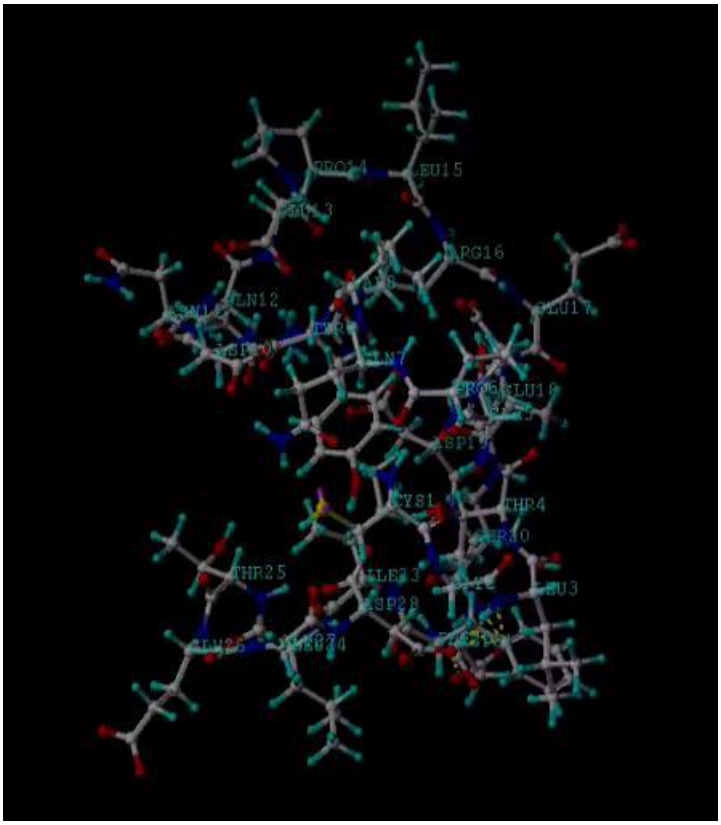

Fig. 23: Peptide 5 in hydrogen bonding with 3-methacrylamido-1-aminium.

Table 9: Summary of the Leapfrog on Peptide 6.

SNO	NAME OF MONOMER	STRUCTURE OF MONOMER	BINDING SCORES K/CAL/MOL
1	3-methacrylamido-1-aminium		-88.14
2	N-3-aminopropylmethacrylamide	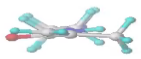	-40.17
3	N,N-methylenebisacrylamide	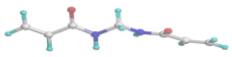	-37.18
4	N-phenylacrylamide	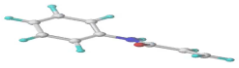	-32.59
5	N-isopropylacrylamide	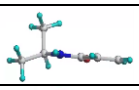	-29.73
6	N-t-butylacrylamide	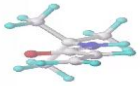	-20.43

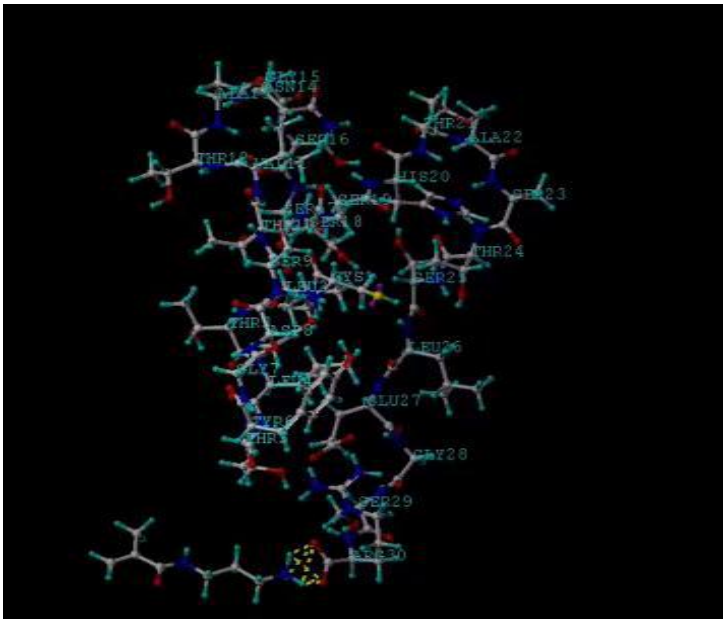

Fig. 24: Peptide 6 in hydrogen bonding with 3-methacrylamido-1-aminium.

DISCUSSION

Tables 4 -9 provides a summary of the results from the leapfrog procedures carried out on the 8 functional monomers against the six peptides. It was observed for the six peptides that, 3-methacrylamido-1-aminium monomer exhibited the highest binding scores with the six peptides. These scores were -72.56 kcal/mol, -64.77 kcal/mol, -68.88 kcal/mol, -77.38 kcal/mol, -108.45 kcal/mol and -88.14 kcal/mol, respectively, an indication of it being the preferred functional monomer for the formation of the molecularly imprinted polymer as a diagnostics tool. It was also observed to have exhibited a high degree of hydrogen bonding with all the peptides as shown in Figs. 19-24. Showing hydrogen bonding with Cysteine-1 in peptide 1; Serine-5 in peptide 2; Leucine-12 in peptide3; Glutamine-2 in peptide 4; Phenylalanine-22 in peptide 5 and Arginine-27 in peptide 6. This is also part of the requirement for the formation of a high affinity, selective and stable molecularly imprinted polymer.

CONCLUSION AND RECOMMENDATION

Crigler Nijjar is a rare genetic disorder caused by the partial or total absence of UGT1A1which is responsible for the metabolism of bilirubin formed in the human body. This causes the yellow coloration of the eyes and with increased levels of bilirubin concentration in certain organs of the body giving rise to several complications which if not well managed can lead to death of neonatals. Results obtained from the eight (8) functional monomers in copulation with the six peptides, one of the functional monomer 3-methacrlylamido-1-aminium showed the highest binding scores with all the peptides with high degree of hydrogen bonding. It was therefore selected as the preferred functional monomer and recommended for use in the synthesis of the molecularly imprinted polymer to be used for the diagnostic tool. We hereby recommend that further work be carried out on this functional monomer which may turn out to be another universal functional monomer like Methacrylic acid (MAA).

REFERENCES

1 Tabandeh I M, Ghassamipour S, Agababa H, Tabatabaei M, Hasheminejad M. Computational design & synthesis MIP for selective extraction of allopurinol from human plasma Jour. Of Chromatogrsphy B, 2012; 898: 24-31.

2 Masque N, Marce R M, Botrull F. Molecularly Imprinted Polymers: new tailor made materials for selective solid-phase extraction. Trends in analytical chemistry, 2001; 20(9): 477–486.

3 Mahony JO, Nolan K, Smyth M R, Mizaikoff B. Molecularly imprinted polymers – potential & challenges in analytical Chemistry. Analytical Chimica Acta, 2005; 534(1): 31-39.

4 Blanco-Lopez M C, Lobocastanon M J. Vottammetric sensor for Vanillymandelic acid based on molecularly imprinted polymer – modified electrodes. Biosensors & Bioelectronics, 2003; 18(4): 353-362.

5 Blanco-Lopez M C, Lobo Castanon A J. Miranda-Ordiere, Turnon – Blanco P. Electro Chemical Sensors based on molecularly imprinted ploymers trac trends in Analytical Chemistry, 2004; 23(1): 36-48.

6 Remcho VT, Tan Z. Molecular Imprinted Polymers recognize specific compounds and show promises as separation media, especially for chiral molecules. Analytical Chemistry, 1999; 71(7): 245-255.

7 Takeuchi T, Haginaka J. Separation and sensing based on molecular recognition using Molecular Imprinted Polymers. Jour. of Chromatography B; Biomedical Sciences & Application, 1999; 728(1): 1-20.

8 Ye L, Haupt K. Molecularly Imprinted Polymers as antibody and receptor mimics for assays, sensors and drug discovery. Analytical & Bioanalytical Chemistry, 2004; 378(8): 1891-1897.

9 Chianella I, Lotierzo M, Piletsky S A, Tothill I E, Chen B N, Karim K, Turner APF. Rational design of a polymer specific for microcristine LR using a Computational approach. Analytical Chemistry, 2002; 74(6): 1288-1293.

10 Piletsky SA, Karim K, Piletska EV, Day CJ, Freebairn KW, Legge C, Turner APF. Recognition of ephedrine enantiomers by molecularly imprinted polymers designed using a computational approach Analyst, 2001; 126(10): 1826-1830.

11 Chianella Iva, Karim Kal, Elena V Piletska, Christopher Pretson, Sergey Piletsky A. Computational design and synthesis of molecularly imprinted polymers with high binding capacity for pharmaceutical applications-model case: adsorbent for abacavir Analytica Chimica Acta, 2006; 559(1): 73-78.

12 Dumitru Pavel, Jolanta Lagowski. Computationally designed monomers and polymers for molecular imprinting of theophylline and it's derivatives:Part 1 Polymer, (2005); 46(18): 7528-7542.

13 Crigler J F, Najjar A. Congenital Familial Nonhemolytic Jaundice with Kernicterus. American Acad. Pediatrics, 1952; 10(2): 169-180.

14 Wolkoff AW, Chowdhury J R, Arias I M. Hereditary Jaundice and Disorder of Metabolic basis of inherited disease/[edited by] John B.Stanbury...[et al.], 1983.

15 Van der Veere C N, Sinaasappel M, McDonagh A F, Rosenthal P, Labrune P, Olievre M, Fevery J, Otte J, McClean P, Bürk G. Current therapy for Crigler – Najjar Syndrome Type 1: Report of a World Registry. Hepatology, 1996: 24(2): 311-315.

16 Strauss K A, Robinson D L, Vreman H J, Puffenberger E G, Hart G, Morton D. H. Management of Hyperbilirubinemia and Prevention of Kernicterus in 20 Patients with Crigler-Najjar Disease. Eur. J. Pediatr, 2006; 165: 306-319.

17 Petit F M, Bézieau S, Gajdos V, Parisot F, Scoul C, Capel L, Stozinic V, Khrouf N, M'rad R. Koshy A. The Tunisian Population History through the Crigler-Najjar type 1 Syndrome. European Journal of Human Genetics, 2008; 16: 848-853.

18 A. Kadakol, S. S. Ghosh, B. S. Sapnal, G. Sharma, J. R. Chowdhury and N. R. Chowdhury,. Genetic Lessons of Bilirubin Uridine Disphophoglucoroonate gluuronostyl transferase (UGTIAI) causing Crigler-Najjar & Gilbert Syndromes: Correlation of genotype to phenotype. Hum. Mutat, 2000; 16: 297-306.

19 Yamamoto K, Sato H, Fujiyama Y, Doida Y, Bamba T. Biochimica et Biophysica Acta. (BBA)-Molecular Basis of Disease, 1998; 1406; 267-273.

20 Crigler-Najjar-syndrome1.jpg. Retrieved from https://www.medindia.net/patients/patientinfo/images/Crigler-Najjar syndrome1.jpg on 15 April, 2019.

21 Gr1.gif.Retrieved from https://www.cell.com/cms/attachment/534197/3683705/gr1.gif on 15 April, 2019.

22 Udomuksorn W, Elliot D J, Lewis B C, Mackenzie P I, Yoovathaworn K, Miners J O. Pharmacogenetics and genomics, 2007; 17: 1017-1029.

23 Gourley G R. In Liver Disease in Children, Third Edition, ed. nonymous, Cambridge University Press, 2007: 270-309.

24 Wennberg R. Unbound bilirubin: a better predictor of Kernicterus. Clin. Chem, (2008); 54: 207-208.

25 Jeffrey Maisels M, Elizabeth Leong. Transcutaneous bilirubin levels in the first 96 hours in a normal new born population of ≥ 35 weeks' gestation. Pediatrics, (2006); 117(4): 1169-1173.

26 Maria Elzbieta Sobaniec-Lotowska, Dariusz Marek Lebensztejn. Ultrastructure of Kupffer cells and hepatocytes in the Dubin-Johnson syndrome: a case report. World Journal of Gastroenterology: WJG, 2006; 12(6): 987.

27 Sergey Piletsky, Elena Piletska, Kal Karim, Graham Foster, Colton Legge. Custom synthesis of molecular imprinted polymers for biotechnological application: Preparation of a polymer selective for tysolin. Analytics Chimica Acta, 2004; 504(1): 123-130.